Exosomes from myeloid derived suppressor cells carry biologically active proteins

Meghan Burke[1], **Waeowalee Choksawangkarn**[1], **Nathan Edwards**[2], **Suzanne Ostrand-Rosenberg**[3], and **Catherine Fenselau**[1]

[1]Department of Chemistry and Biochemistry, University of Maryland, College Park MD 20742

[2]Department of Biochemistry and Molecular & Cellular Biology, Georgetown University Medical Center, Washington DC, 20057

[3]Department of Biological Sciences, UMBC, Baltimore MD, 21250

Abstract

Myeloid-derived suppressor cells (MDSC) are present in most cancer patients where they inhibit natural anti-tumor immunity and are an obstacle to anti-cancer immunotherapies. They mediate immune suppression through their production of proteins and soluble mediators that prevent the activation of tumor-reactive T lymphyocytes, polarize macrophages towards a tumor-promoting phenotype, and facilitate angiogenesis. The accumulation and suppressive potency of MDSC is regulated by inflammation within the tumor microenvironment. Recently exosomes have been proposed to act as intercellular communicators, carrying active proteins and other molecules between sender cells and receiver cells. In this report we describe the proteome of exosomes shed by MDSC induced in BALB/c mice by the 4T1 mammary carcinoma. Using bottom-up proteomics, we have identified 412 proteins. Spectral counting identified 63 proteins whose abundance was altered > 2-fold in the inflammatory environment. The pro-inflammatory proteins S100A8 and S100A9, previously shown to be secreted by MDSC and to be chemotactic for MDSC, are abundant in MDSC-derived exosomes. Bioassays reveal that MDSC-derived exosomes polarize macrophages towards a tumor-promoting type 2 phenotype, in addition to possessing S100A8/A9 chemotactic activity. These results suggest that some of the tumor-promoting functions of MDSC are implemented by MDSC-shed exosomes.

Introduction

Exosomes (1–3) are present in high abundance in the tumor microenvironment where they transfer information between cells (4). Exosomes of tumor origin stimulate apoptosis of tumor-reactive T cells, induce immune suppressive myeloid-derived suppressor cells (MDSC), promote angiogenesis, and exchange genetic material between cells (5–10). Increased understanding of the mechanisms that activate anti-tumor immunity, combined with promising therapeutic strategies in some cancer patients and experimental animals have led to enthusiasm for immunotherapy as a treatment for established cancers. Despite limited recent successes, active immunotherapy has not been widely effective (11). The lack of

This information is available free of charge via the Internet at http://pubs.acs.org

efficacy is attributed in large part to immune suppressive cells present in most cancer patients (12, 13). MDSC are present in virtually all cancer patients and experimental animals with cancer and are considered one of the dominant cell populations that obstructs immunotherapy (14, 15). MDSC inhibit anti-tumor immunity by preventing the activation of tumor-reactive T lymphocytes, by inhibiting T lymphocyte trafficking to sites where they could be activated (16), and by polarizing macrophages towards a tumor-promoting phenotype (17). Some of these mechanisms require cell-to-cell-interactions between MDSC and the target cells, and in some cases, the release of soluble mediators. Identification of the molecules regulating these processes could lead to drug interventions for preventing MDSC-mediated suppression. In vivo, the development of MDSC tracks with the level of inflammation, with increasing inflammation enhancing the potency and quantity of MDSC (18, 19). Exosomes, as extracellular messengers, may contribute to the differences in MDSC abundance and suppressive activity under heightened inflammatory conditions

We now report that MDSC isolated from BALB/c mice carrying 4T1 mammary carcinomas shed exosomes that contain proteins derived from many subcellular compartments and are associated with diverse functions. The protein cargo of MDSC-derived exosomes appears to be regulated by the extent of inflammation in which the MDSC develop *in vivo*. Importantly, MDSC-shed exosomes polarize macrophages towards a tumor-promoting phenotype and drive MDSC chemotaxis, suggesting that MDSC-derived exosomes play an important role as communicators in the tumor microenvironment.

Experimental

Myeloid-derived suppressor cells

BALB/c mice were injected in the mammary fat pad with 7000 wild type 4T1 mammary carcinoma cells or 4T1 cells stably transfected and expressing interleukin-1β (IL-1β) as described. When tumors were greater than ~8 mm in diameter (~3–4 weeks after initial inoculation), MDSC were harvested from the blood and monitored by immunofluorescence and flow cytometry for purity by expression of the MDSC markers Gr1 and CD11b (Figure 1) (18). MDSC used in experiments were >90% Gr1$^+$CD11b$^+$. MDSC induced by wild type 4T1 and 4T1/IL-1β tumor cells are termed "conventional" and "inflammatory" MDSC, respectively. All procedures with animals and animal-derived materials were approved by the UMBC and UMCP Institutional Aminal Care and Use Committees.

Exosomes

Purified MDSC obtained from 2–3 mice (~1×10^8 MDSC for each experiment) were plated at 4×10^6 cells/ml in serum-free HL-1 medium (BioWhittaker, Walkersville, MD) and maintained at 37° C with 5% A CO_2. After 16 hrs the cultures were centrifuged at 805 g for 5 min (Eppendorf 5810R centrifuge), the pellets discarded, and the supernatants centrifuged at 2090 g for 30 min (Sorvall RC5C, SS34 rotor). The supernatants were then ultracentrifuged (Beckman L8 ultracentrifuge) at 100,000 g for 20 hrs at 10° C using an SW40Ti rotor. Supernatants were discarded and the pellets containing the exosomes were resuspended in PBS and absorbances were measured at 260 and 280 nm. Protein content was assayed by Bradford Quick Start according to the manufacturer's directions (Biorad). Exosomes were stored at −80° C until used. For migration experiments, exosomes were resuspended to the original volume of the conditioned medium from which they were obtained so a direct comparison of the effects of exosomes versus conditioned medium could be made. For the MDSC-macrophage cross-talk experiments, exosomes were used at 1x, 2.5x, and 5x concentrations. On average, one ml of conditioned medium contained 714 μg of exosomal protein.

Sucrose density gradient fractionation of exosomes

Freshly prepared ultracentrifuged exosomes were resuspended in 1.8 to 2.0 ml of 2.5M sucrose/0.020 M Hepes and layered on the bottom of $9/16'' \times 3 ¾''$ polyallomer ultracentrifuge tubes (Beckman). A 10 ml gradient of 0.25 M to 2.0 M sucrose in 0.020M Hepes was then layered over the 2 ml containing the exosomes for a total volume of 11.8 to 12 ml. Gradients were ultracentrifuged (Beckman L8 ultracentrifuge) at 10° C for 16 hrs at 100,000g in an SW40Ti rotor. One half ml fractions were collected and assessed by optical density (Figure 1). Density of the fractions was confirmed by refractometry.

Transmission electron micrographs

An aliquot containing 0.03–0.3 pg exosomes suspended in 2% glutaraldehyde was applied to a Formvar-coated grid and negatively stained with uranyl acetate. Electron micographs were acquired using a Zeiss EM10 transmission electron microscope at an accelerating voltage of 80keV.

Protein analysis

Aliquots of conventional and inflammatory exosomes containing 25 µg of total protein were lysed in 8 M urea. Fifty mM ammonium bicarbonate was added to each sample to dilute the final urea concentration to 0.8 M, which is compatible with tryptic digestion. Each sample was then reduced in 20 mM DTT at 56 °C for 30 minutes followed by alkylation in 40 mM iodoacetamide at room temperature in the dark for 30 minutes. Three technical replicates of 7 µg total protein were analyzed by LC-MS/MS (using HPLC MS/MS parameters outlined below) for three biological replicates each for conventional and inflammatory exosomes.

HPLC MS/MS Analysis

LC-MS/MS analyses were performed on a Shimadzu Prominent nanoHPLC (Shimadzu BioSciences, Columbia MD) in-line with an LTQ-orbitrap XL (Thermo Fisher Scientific, San Jose, CA). Peptides prepared via tryptic digestion were injected onto an Acclaim PepMap 300 C18 precolumn (Dionex, Sunnyvale, CA) followed by desalting by 10% Solvent A (97.5% H_2O, 2.5% ACN, and 0.1% formic acid) for 20 minutes. Peptides were fractionated on a C-18 analytical column (Grace Vydak, Deerfield IL) with a linear gradient increasing from 0 to 40% solvent B (97.5% ACN, 2.5% H_2O, and 0.1% formic acid) in 170 minutes, followed by an increase from 40 to 85% solvent B in 40 minutes. Flow rate was 500 nL/min. Precursor scans were acquired in the orbitrap with a resolution of 30,000 at m/z 400. In each cycle the nine most abundant ions were selected for fragmentation by collisional induced dissociation (CID), and product ion scans were acquired in the LTQ. A dynamic exclusion of 1 repeat count over 180 seconds was used.

Bioinformatics

Peptides and proteins were identified by the PepArML meta-search engine (20) using the mouse reference proteome of the UniProtKnowledgeBase (June 2013) containing 50,807 sequences. Carbamidomethylation of cysteine was selected as a fixed modification and oxidation of methionine and deamidation of asparagine and glutamine residues were selected as variable modifications. Peptide identifications from technical and biological replicates were pooled and filtered at 1% (spectral) FDR, as computed by PepArML using the method of Elias and Gygi (21), and identified proteins required to contain at least two distinct, unshared peptides, ensuring protein FDR of at most 0.01%. Spectral counts for identified proteins, spectral count ratios (R_{SC}) as described in Old et al. (22), and statistical significance for differential spectral counts determined using in house software. Differential spectral count *p*-values were computed using the Fisher exact-test, and corrected for multiple testing by transformation to false-discovery-rate (FDR) using the method of

Benjamini and Hochberg (23). Identified proteins are assigned to cellular components according to their Gene Ontology annotations and the PIR GO Slim.

MDSC chemotaxis

Cells used in the chemotaxis assay were >90% $Gr1^+CD11b^+$ conventional MDSC as assessed by flow cytometry (24). Five hundred µl of fresh media, media from MDSC cultures (conditioned media), or MDSC-derived exosomes from the equivalent amount of conditioned medium in fresh media were placed in individual wells of 24 well plates (lower compartment). Monoclonal antibodies to S100A8, S100A9, or irrelevant control isotype matched antibodies (10 µg/500 µl; Santa Cruz Biotech) were included in some wells. Transwells with an 8µm polycarbonate semi-permeable membrane were then inserted in each well and 1×10^6 MDSC in 100 µl of serum-free IMDM medium were placed in the transwells (upper compartment). Assembled transwells were incubated at 37° C in 5% CO_2 for 3hrs, and the MDSC in the bottom chamber were then quantified by hemocytometer. Values for each sample are the average results of duplicate samples and three independent hemocytometer counts per well (25).

MDSC-macrophage cross-talk

BALB/c mice were injected intraperitoneally with 1 ml of 3% thioglycolate and peritoneal exudate cells (PEC) harvested 4 days later. Percent of macrophages in the exudate was determined by flow cytometry analysis of the macrophage markers F4/80 and CD11b. PEC were plated in 24 well plates at 7.5×10^5 $F4/80^+CD11b^+$ cells/well/500 µl DMEM medium supplemented with 10% fetal bovine serum and incubated at 37° C in 5% CO_2 for 3hrs. Non-adherent cells (non-macrophages) were then removed and the attached macrophages were washed with macrophage medium (DMEM/5% serum). Five hundred µl of macrophage medium containing 7.5×10^5 conventional MDSC (>90% $Gr1^+CD11b^+$ cells) or MDSC-derived exosomes from 7.5×10^5 (1X), 18.7×10^5 (2.5X), or 37.5×10^5 (5X) MDSC were then added to each well. MDSC and macrophages were activated with IFNγ and LPS and co-cultured at a ratio of 1:1 (5×10^5 cells of each type/200 µl/well) for 18 hours. Supernatants were harvested and assayed by ELISA for IL-12 (19).

Results and Discussion

The techniques most widely used for characterization of exosomes are density measurements and imaging by transmission electron microscopy. The vesicles shed by both conventional and inflammatory MDSC (Figure 1A) exhibited densities between 1.2 and 1.3 g/mL (Figure 1B) (1, 3, 26). Transmission electron micrographs of this material revealed vesicles with diameters 25–30 nm (Figure 2), within the range ascribed to exosomes (1–3, 26). It should be noted that the MDSC that shed these small exosomes are smaller than most eukaryotic cells (35). The negative control shown in Figure 2 indicates that structures of 15 nm in diameter are artifacts of TEM sample preparation.

Exosomal protein was used as an indicator of the number of exosomes, and was normalized for the number of MDSC cells used in each preparation in order to compare the amount of exosomes shed by conventional MDSC and inflammatory MDSC. The ratio, expressed as exosomal protein (µg) per MDSC cell, at the end of 16 hr was $[1.1 \pm 0.1] \times 10^{-6}$ (n=4) and $[1.2 \pm 0.2] \times 10^{-6}$ (n=4) for conventional and inflammatory MDSC, respectively. The similar ratios demonstrate that conventional and inflammatory MDSC shed exosomes with approximately the same frequency.

Three hundred and eighty seven proteins were identified (from 2528 peptides) in exosomes from conventional MDSC (Supplemental Table 1), and 374 proteins were identified (from 2280 peptides) in exosomes from inflammatory MDSC (Supplemental Table 1). When the

two inventories are combined, 412 proteins were identified. Mathivanan and Simpson (27) established ExoCarta as a database of proteins reported from analyses of different exosome proteomes. About 83% of the proteins identified in exosomes from MDSC are in ExoCarta (August 2013). A searchable website EVpedia has been created by Kim et al (28) for exosomal proteins. About 87% of the proteins identified here are also listed in EVpedia (August 2013). A third database, Vesiclepedia, has recently been established for all extracellular vesicles (29). Among proteins identified in our exosomes, 93% are listed in Vesiclepedia (August 2013). Exosomal proteins from the inventory that have not previously been reported in ExoCarta, EVpedia, or Vesiclepedia are shown in Supplemental Table 2.

Annexins (A1, A2, A3, A6, A7, A11) and tetraspanins, including CD177, were identified along with GTPases, NCK microfibrils (NCK associated protein 1 like), cytoskeletal proteins, VSP35 (a member of the ESCRT complex), heat shock cognate 71 kDa protein, heat shock 70 kDa protein 4, and HSP90 alpha and beta, all proteins reported to be characteristic of exosomes (30).

A suite of subunits from the 26S proteasome was present, including 26S protease regulatory subunit 6A, 26S proteasome non-ATPase regulatory subunits 1,2,5,6,7,11, and 13, proteasome subunit beta type-2 and proteasome subunit alpha type-6. This raises the possibilities that the proteasome may be carried by these exosomes, or that the disassembled proteasome is removed from the cell by these exosomes.

More than a dozen histone variants were detected, as well as several elongation factors (1-gamma, 1-alpha 1, and 2), DNA topoisomerase, RNA helicase (ATP-dependent RNA helicase DDX39A) and a zinc finger (DBF-type zinc finger-containing protein 2 homolog). The presence of these and other nucleic acid binding proteins is consistent with reports that exosomes can alter protein expression in receiver cells (5,7, 9–11,12, 31,32).

Metabolic enzymes were identified from the pentose phosphate pathway responsible for synthesis of NADPH and ribose-5-phosphate including: glucose-6-phosphate 1-dehydrogenase X, 6-phosphogluconate dehydrogenase and transketolase. Most of the enzymes in the glycolysis and gluconeogenesis pathways were present: pyruvate kinase PKM, glucose-6-phosphate isomerase, glyceraldehyde-3-phosphosphate dehydrogenase, alpha-enolase, L-lactate dehydrogenase A chain, fructose-bisphosphate aldolase, phosphoglycerate kinase 1, glycogen phosphorylase liver form and glycogenin-1. These proteins are also listed in databases of proteins identified in various kinds of exosomes.

Several proteins relevant to the immune system were also identified. S100A8 and S100A9 are known (25, 33) to drive chronic and acute inflammation. Myeloid bactecin strongly interacts with immune cells and participates in the inflammatory response (34).

Figure 3 summarizes the sub-cellular locations of the exosomal proteins identified, and compares them with a set of 305 proteins identified (35) in a whole cell lysate of conventional MDSC. Exosomes from both conventional and inflammatory MDSC contain proteins residing in the major intracellular organelles and the distribution of proteins in both samples is similar. Compared to the whole cell lysate, a lower percentage of exosomal proteins are assigned to the parental cell nucleus and endoplasmic reticulum.

Chronic inflammation in the tumor microenvironment increases the quantity and suppressive potency of the parental MDSC (18, 19), and is associated with altered concentrations of some proteins in MDSC (35). In the exosomes shed by MDSC spectral counting was used to compare protein abundances. Out of 412 proteins quantified in conventional and inflammatory samples (See Supplementary Table 1) the abundances of 63 proteins differed by more than two fold with FDR less than 0.05. Heightened inflammation is associated with

decreased abundances of 33 proteins in exosomes, including several proteins that participate in the innate immune response: ficolin-1, C4b-binding protein, chitinase-3-like protein 3, complement C3, and CD5 antigen-like. Other proteins that decreased with heightened inflammation include cytoskeletal proteins (spectrin beta 1, ankyrin-1, tubulin beta-1 chain and nesprin-1) and chemotactic proteins (myeloid cysteine-rich protein and platelet factor 4), suggesting a change in exosome migration.

Thirty proteins increased in abundance under heightened inflammatory conditions, including GTP and ATP binding proteins (ATP-citrate synthase, ADP-ribosylation factor 1, and phosphatidylinositol 4-phosphate 3-kinase C2 domain containing subunit gamma). Interestingly, the coatomer subunit beta, recruited by ADP-ribosylation factors that participate in membrane curvature and budding (36) is increased more than 2 fold with inflammation. Other proteins that increase include biosynthetic proteins (serine-tRNA ligase cytoplasmic, valine-tRNA ligase, aminopeptidase B, fatty acid synthase, ATP-citrate synthase, and elongation factor 1-gamma) and the retromer component vacuolar protein sorting-associated protein 35, which participates in protein sorting (37).

The relative abundance of proteins S100 A8 and A9 did not change in exosomes shed from MDSC due to inflammation. These are usually present as the A8/A9 heterodimer, a pro-inflammatory mediator that is present at sites of inflammation. It was previously shown to be chemotactic and induce migration of MDSC to tumor sites (25, 33). It also stimulates polarization of macrophages towards the tumor-promoting M2 phenotype (17). These functions have previously been attributed to the extracellular secretion of S100A8/A9 by MDSC themselves and by tumor cells. To test the possibility that exosomes carrying S100A8/A9 are responsible for these effects, bioassays were conducted with intact MDSC, MDSC-derived exosomes, and macrophages.

Chemotactic activity was assessed by co-culturing intact MDSC and MDSC-derived exosomes on opposite sides of a semi-permeable membrane and measuring the number of MDSC migrating through the membrane towards the exosomes (Figure 4). Exosomes were chemotactic for intact MDSC and chemotaxis was significantly inhibited if antibodies to S100A8 or S100A9 were included with the exosomes. The chemotaxis was specific since inclusion of an irrelevant isotype matched antibody did not prevent migration. These results indicate that MDSC-derived exosomes mediate chemotaxis through their content of S100A8 and A9. The same assay has been previously applied to conditioned media (25), where antibodies to S100 A8 and A100 A9 reduced migration by amounts similar to what is reported here for exosomes. In the current assay, exosomes were >90% as chemotactic as the equivalent amount of conditioned medium, indicating that most of the S100 A8/A9 activity is contained in exosomes.

One of the suppressive mechanisms used by MDSC to promote tumor progression is their conversion of macrophages from tumoricidal cells (so-called M1 macrophages) to cells that facilitate tumor growth (so-called M2 macrophages). This conversion involves the switching off of macrophage production of IL-12, a cytokine that drives the development of tumoricidal T lymphocytes and natural killer cells (17). To determine if this function is mediated by MDSC-derived exosomes, M1 macrophages were co-cultured with either intact MDSC or exosomes derived from an equal number of MDSC or multiples thereof (2.5X, 5X). Macrophage production of IL-12 was measured by ELISA (Figure 5). MDSC-derived exosomes decreased IL-12 production; however, on a per cell basis they are less effective than intact MDSC. These results indicate that exosomes contribute to the ability of MDSC to polarize macrophages; however non-exosome mechanisms are also involved.

Conclusions

Exosomes shed by myeloid-derived suppressor cells are rich in proteins. Exosomal proteins, unlike RNA, can have an immediate effect on the target cell, making the exosomal proteome a valuable source of information about intracellular communication in the tumor microenvironment. Their cargo includes many histones, enzymes active in energy metabolism, proteasome subunits and the pro-inflammatory mediators S100A8 and S100A9. Neither the number of exosomes shed per cell nor the concentration of protein S100 A8 in the exosomes varies significantly between MDSC isolated from low and high inflammatory murine environments. Biological assays demonstrate both autocrine and paracrine activities for these exosomes and demonstrate causality for S100A8 and S100A9. These results demonstrate that some of the immune suppressive activity of MDSC is mediated by MDSC-shed exosomes. Since MDSC infiltrate solid tumors and also circulate in the blood and are present in the bone marrow, MDSC-derived exosomes may function as short and long-range mediators to regulate anti-tumor immunity and facilitate tumor growth.

Supplementary Material

Refer to Web version on PubMed Central for supplementary material.

Acknowledgments

References

1. Shen B, Wu N, Yang JM, Gould SJ. Protein targeting to exosomes/microvesicles by plasma membrane anchors. J Biol Chem. 2011; 286:14383–14395. [PubMed: 21300796]

2. Choi DS, Yang JS, Choi EJ, Jang SC, Park S, Kim OY, Hwang D, Kim KP, Kim YK, Kim S, Gho YS. The Protein Interaction Network of Extracellular Vesicles Derived from Human Colorectal Cancer Cells. J Prot Res. 2012; 11:1144–1151.

3. Gould SJ, Raposo G. As we wait: coping with an imperfect nomenclature for extracellular vesicles. J Extracellular Vesicles. 2013; 2:1–3.

4. Johnstone RM. Exosomes biological significance: A concise review. Blood Cells, Molecules and Diseases. 2006; 36:315–321.

5. Simpson RJ, Lim JW, Moritz RL, Mathivanan S. Exosomes: proteomic insights and diagnostic potential. Expert Reviews. 2009; 6:267–283.

6. Iero M, Valenti R, Huber V, Filipazzi P, Parmiani G, Fais S, Rivoltini L. Tumour-released exosomes and their implications in cancer immunity. Cell Death and Differentiation. 2008; 15:80–88. [PubMed: 17932500]

7. Valadi H, Ekstrom K, Bossios A, Sjostrand M, Lee JJ, Lotvall JO. Exosome-mediated transfer of mRNAs and microRNAs is a novel mechanism of genetic exchange between cells. Nat Cell Biol. 2007; 9:654–659. [PubMed: 17486113]

8. Xiang X, Poliakov A, Liu C, Liu Y, Deng Z, Wang J, Cheng Z, Shah SV, Wang G, Zhang L, Grizzle WE, Mobley J, Zhang H. Induction of myeloid-derived suppressor cells by tumor exosomes. Int J Cancer. 2009; 124:22621–2633.

9. Skog J, Wurdinger T, van Rijn S, Meijer D, Gainche L, Sena-Esteves M, Curry ST, Carter RS, Krichevesky AM, Breakefield XO. Glioblastoma microvesicles transport RNA and protein that promote tumor growth and provide diagnostic biomarkers. Nat Cell Bio. 2008; 10:1470–1476. [PubMed: 19011622]

10. Balaj L, Lessard R, Dai L, Cho Y, Pomeroy SL, Breakefield XO, Skog J. Tumour microvesicles contain retrotransposon elements and amplified oncogene sequences. Nature Commun. 2011; 2:180.10.1038/ncomms1180 [PubMed: 21285958]

11. Lesterhuis WJ, Haanen JB, Punt CJ. Cancer immunotherapy--revisited. Nature Rev Drug Discovery. 2011; 10:591–600.

12. Schreiber RD, Old LJ, Smyth MJ. Cancer immunoediting: integrating immunity's roles in cancer suppression and promotion. Science. 2011; 331:1565–1570. [PubMed: 21436444]

13. Poschke I, Mougiakakos D, Kiessling R. Camouflage and sabotage: tumor escape from the immune system. Cancer Immunol Immunother. 2011; 60:1161–1171. [PubMed: 21626032]

14. Gabrilovich DI, Nagaraj S. Myeloid-derived suppressor cells as regulators of the immune system. Nature Rev Immunol. 2009; 9:162–174. [PubMed: 19197294]

15. Marx J. Cancer immunology. Cancer's bulwark against immune attack: MDS cells. Science. 2008; 319:154–156. [PubMed: 18187637]

16. Hanson EM, Clements VK, Sinha P, Ilkovitch D, Ostrand-Rosenberg S. Myeloid-derived suppressor cells down-regulate L-selectin expression on CD4+ and CD8+ T cells. J Immunol. 2009; 183:937–944. [PubMed: 19553533]

17. Ostrand-Rosenberg S. Myeloid-derived suppressor cells: more mechanisms for inhibiting antitumor immunity. Cancer Immunol Immunother. 2010; 59:1593–1600. [PubMed: 20414655]

18. Bunt SK, Sinha P, Clements VK, Leips J, Ostrand-Rosenberg S. Inflammation induces myeloid-derived suppressor cells that facilitate tumor progression. J Immunol. 2006; 176:284–290. [PubMed: 16365420]

19. Bunt SK, Yang L, Sinha P, Clements VK, Leips J, Ostrand-Rosenberg S. Reduced inflammation in the tumor microenvironment delays the accumulation of myeloid-derived suppressor cells and limits tumor progression. Cancer Res. 2007; 67:10019–10026. [PubMed: 17942936]

20. Edwards N, Wu X, Tseng CW. An unsupervised, model-free, machine-learning combiner for peptide identifications from tandem mass spectra. Clinical Proteomics. 2009; 5:23–36.

21. Elias JE, Gygi SP. Target-decoy search strategy for increased confidence in large-scale protein identifications by mass spectrometry. Nat Methods. 2007; 4:207–214. [PubMed: 17327847]

22. Old WM, Meyer-Arendt K, Aveline-Wolf L, Pierce KG, Mendoza A, Sevinsky JR, Resing KA, Ahn NG. Comparison of label-free methods for quantifying human proteins by shotgun proteomics. Mol Cell Prot. 2005; 4:1487–1502.

23. Benjamini Y, Hochberg Y. Controlling the false discovery rate: A practical and powerful approach to multiple testing. J Royal Statistical Soc Series B (Methodological). 1995; 57:289–300.

24. Sinha P, Clements VK, Ostrand-Rosenberg S. Reduction of myeloid-derived suppressor cells and induction of M1 macrophages facilitate the rejection of established metastatic disease. J Immunol. 2005; 174:636–645. [PubMed: 15634881]

25. Sinha P, Okoro C, Foell D, Freeze HH, Ostrand-Rosenberg S, Srikrishna G. Proinflammatory S100 proteins regulate the accumulation of myeloid-derived suppressor cells. J Immunol. 2008; 181:4666–4675. [PubMed: 18802069]

26. Thery C, Zitvogel L, Amigorene S. Exosomes: composition, biogenesis and function. Nat Rev Immunol. 2002; 2:569–579. [PubMed: 12154376]

27. Mathivanan S, Simpson RJ. ExoCarta: A compendium of exosomal proteins and RNA. Proteomics. 2009; 9:4997–5000. [PubMed: 19810033]

28. Kim D, Kang B, Kin O, Choi D, Lee J, Kim SR, Go G, Yoon YJ, Kim JH, Jang SC, Park K, Choe E, Kim KP, Desiderio DM, Kim Y, Lotvall J, Hwang D, Gho YS. EVpedia: an integrated database of high-throughput data for systemaic analyses of extracellular vesicles. J Extracellular Vesicles. 2013; 2:20384.

29. Kalra H, Simpson RJ, Ji H, Aikawa E, Altevogt P, Askenase P, Bond VC, Borràs FE, Breakefield X, Budnik V, Buzas E, Camussi G, Clayton A, Cocucci E, Falcon-Perez JM, Gabrielsson S, Gho YS, Gupta D, Harsha HC, Hendrix A, Hill AF, Inaal JM, Jenster G, Kiang LS, Krämer-Albers EM, Llorente A, Lötvall J, Mincheva-Nilsson L, Nazarenko I, Nieuwland R, Nolte-'t Hoen ENM, Pandey A, Patel T, Piper MG, Pluchino S, Prasad TSK, Rajendran L, Raposo G, Record M, Reid GE, Sánchez-Madrid F, Schiffelers RM, Siljander P, Stoorvogel W, Taylor D, Thery C, Valadi H, van Balkom BWM, Vázquez J, Vidal M, Yáñez-Mó M, Zoeller M, Mathivanan S. Vesiclepedia: A

compendium for extracellular vesicles with continuous community annotation. PLoS Biology. 2012; 12:e1001450. [PubMed: 23271954]

30. Mathivanan S, Ji H, Simpson RJ. Exosomes: Extracellular organelles important in intercellular communication. J Proteomics. 2010; 73:1907–1920. [PubMed: 20601276]

31. Skog J, Würdinger T, van Rijn S, Meijer DH, Gainche L, Sena-Esteves M, Curry WT Jr, Carter BS, Krichevsky AM, Breakefield XO. Glioblastoma microvesicles transport RNA and proteins that promote tumour growth and provide diagnostic biomarkers. Nat Cell Biol. 2008; 10:1470–1476. [PubMed: 19011622]

32. Taylor DD, Gercel-Taylor CG. Tumour-derived exosomes and their role in cancer-associated T-cell signaling defects. Brit J Cancer. 2005; 92:305–311. [PubMed: 15655551]

33. Cheng P, Corzo CA, Luetteke N, Yu B, Nagaraj S, Bui MM, Ortiz M, Nacken W, Sorg C, Vogl T, Roth J, Gabrilovich DI. Inhibition of dendritic cell differentiation and accumulation of myeloid-derived suppressor cells in cancer is regulated by S100A9 protein. J Exp Med. 2008; 205:2235–2249. [PubMed: 18809714]

34. Soehnlein O, Weber C, Lindbom L. Neutrophil granule proteins tune monocytic cell function. Trends Immunol. 2009; 30:538–546. [PubMed: 19699683]

35. Choksangakarn, W. PhD thesis. University of Maryland; 2009. Development of a Proteomic Strategy for Analysis of Plasma Membrane Proteins.

36. Graham TR, Kozlov MM. Interplay of proteins and lipids in generating membrane curvature. Curr Opin Cell Bio. 2010; 22:430–436. [PubMed: 20605711]

37. Saftig P, Klumperman J. Lysosome biogenesis and lysosomal membrane proteins: trafficking meets function. Nature Rev Mol Cell Biol. 2009; 10:623–635. [PubMed: 19672277]
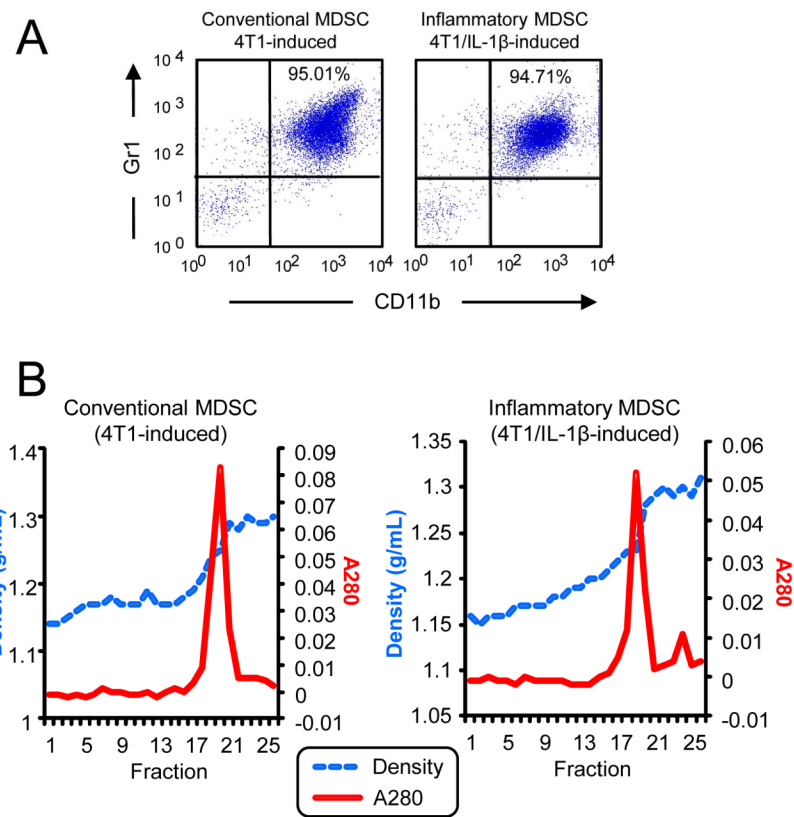
Figure 1.
A: Flow cytometry profile of MDSC expression for Gr1 and CD11b. B: Sucrose density (g/mL) and optical density (OD 280) plots of fractions from sucrose density gradients containing exosomes from conventional (left) and inflammatory (right) MDSC.
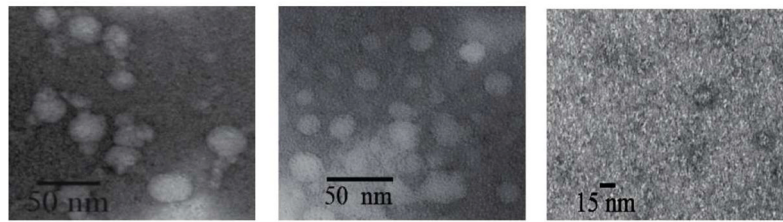
Figure 2.
Transmission electron microscope images of (left) exosomes shed by conventional MDSC; (middle) exosomes shed by inflammatory MDSC; the TEM stain itself (right).
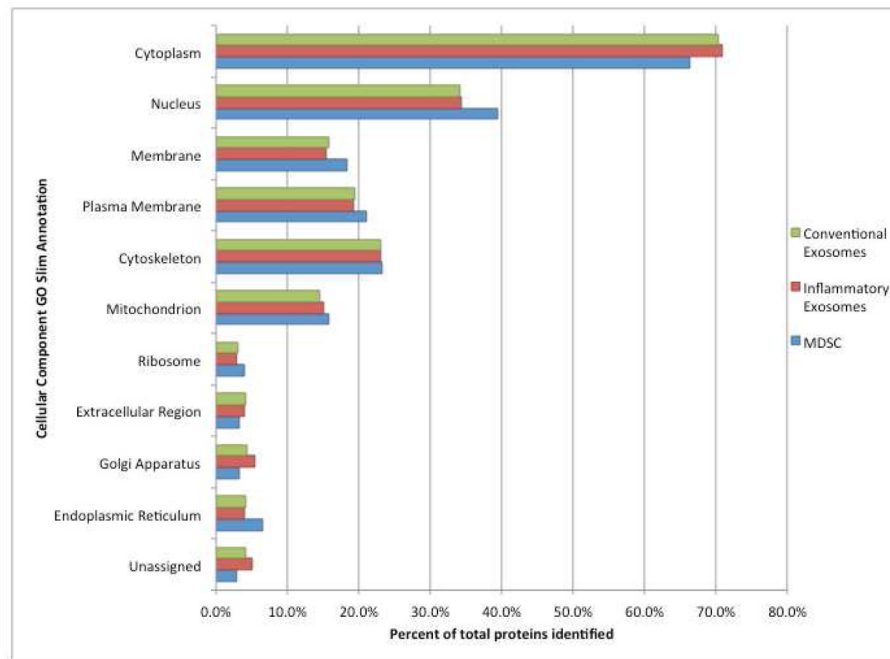
Figure 3.
Intracellular protein locations assigned by Gene Ontology annotations and the PIR GO Slim. Green: from exosomes from conventional MDSC; Red: from exosomes from inflammatory MDSC; Blue: from lysate (35) of conventional MDSC.
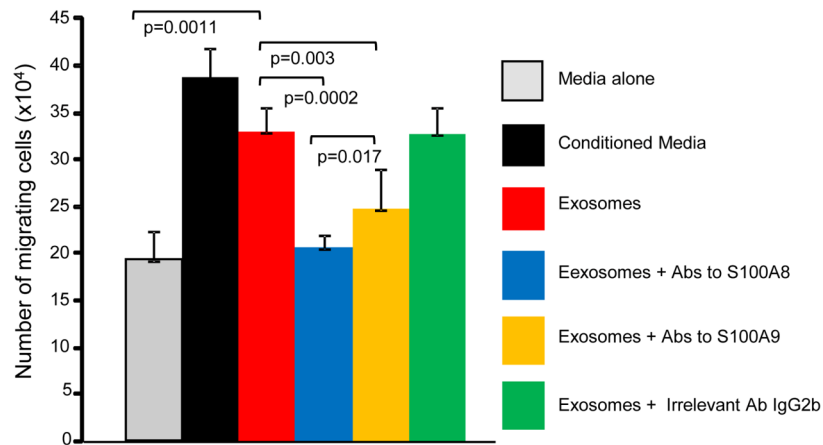
Figure 4.
Exosomes shed by MDSC contain S100A8 and S100A9 proteins that are chemotactic for MDSC. MDSC were placed in the upper compartment of transwells and either tumor-conditioned medium or MDSC shed exosomes ± antibodies to S100A8 or S100A9 were placed in the lower compartment. The number of MDSC migrating to the lower compartment was determined after 3 hrs of incubation. Values are the average ± SD of 3 independent cell counts of duplicate samples. The concentration of purified exosomes is equivalent to the concentration of exosomes in conditioned medium.

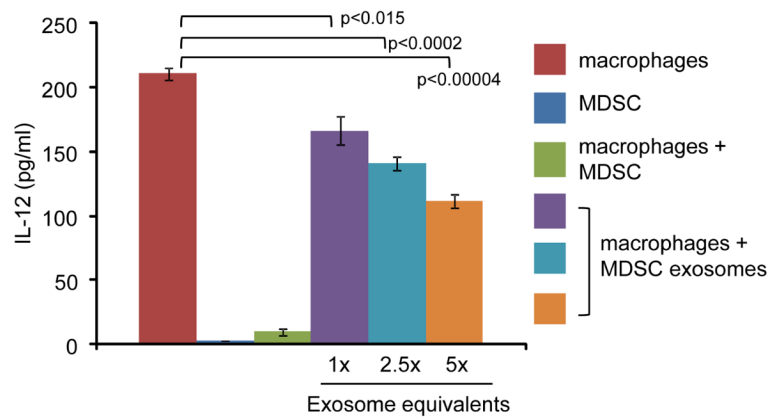**Figure 5.**
Exosomes shed by MDSC polarize macrophages from a tumoricidal M1 phenotype to a tumor-promoting M2 phenotype by inhibiting macrophage production of IL-12. Type 1 macrophages were co-cultured alone, or in the presence of intact MDSC or exosomes derived from either an equal number of MDSC (1X) or multiples thereof. shed by MDSC. IL-12 production by macrophages was measured by ELISA.

Table 1

Proteins with significantly greater abundance in conventional exosomes (R_{sc} 1 and FDR   0.05). R_{sc} is reported as the $\log_2$ ratio of conventional versus inflammatory exosomes.

Accession	Protein	R_{sc}	FDR
P70390	Short stature homeobox protein 2	8.6	6.26E-157
P04919	Band 3 anion transport protein	6.4	5.05E-32
P08032	Spectrin alpha chain, erythrocytic 1	5.6	7.16E-19
Q8CIZ8	von Willebrand factor	4.8	3.56E-10
P08226	Apolipoprotein E	4.6	5.86E-09
Q61171	Peroxiredoxin-2	4.4	1.53E-07
Q9QUM0	Integrin alpha-IIb	4.3	6.14E-07
P01837	Ig kappa chain C region	3.7	1.28E-04
P29788	Vitronectin	3.3	1.50E-03
P49722	Proteasome subunit alpha type-2	3.3	1.50E-03
Q02357	Ankyrin-1	3.3	1.50E-03
Q3UGX2	Spectrin beta 1	3.3	1.50E-03
Q8K482	EMILIN-2	3.3	1.50E-03
Q9QWK4	CD5 antigen-like	3.0	9.63E-03
Q07797	Galectin-3-binding protein	2.8	1.74E-02
P11276	Fibronectin	2.7	3.08E-124
O70165	Ficolin-1	2.7	2.95E-02
P08607	C4b-binding protein	2.6	4.68E-03
P10605	Cathepsin B	2.5	8.26E-03
P07724	Serum albumin	2.5	7.87E-22
Q61646	Haptoglobin	2.1	1.08E-03
P01872	Ig mu chain C region secreted form	2.1	7.19E-13
O35744	Chitinase-3-like protein 3	2.0	8.90E-05
P35441	Thrombospondin-1	1.9	4.55E-14
Q6ZWR6	Nesprin-1	1.9	1.54E-02
P62259	14-3-3 protein epsilon	1.5	6.12E-03
P82198	Transforming growth factor-beta-induced protein ig-h3	1.5	1.04E-02
Q8C2Q7	Heterogeneous nuclear ribonucleoprotein H	1.5	4.89E-02
A2AQ07	Tubulin beta-1 chain	1.5	1.88E-03
P01027	Complement C3	1.3	4.62E-08
Q8K426	Myeloid cysteine-rich protein	1.3	2.59E-02
Q9Z126	Platelet factor 4	1.1	4.71E-03
Q9R1P3	Proteasome subunit beta type-2	1.0	2.41E-02

Table 2

Proteins with significantly greater abundance in inflammatory exosomes (Rsc 1 and FDR 0.05). R_{sc} is reported as the $\log_2$ ratio of inflammatory versus conventional exosomes.

Accession	Protein	RSC	FDR
Q5SS00	DBF4-type zinc finger-containing protein 2 homolog	3.6	1.48E-03
Q8VDP4	DBIRD complex subunit KIAA1967 homolog	3.1	1.39E-02
E9QQ35	Phosphatidylinositol 4-phosphate 3-kinase C2 domain- containing subunit gamma	3.1	1.10E-03
P12970	60S ribosomal protein L7a	3.0	2.29E-02
P84078	ADP-ribosylation factor 1	3.0	2.29E-02
P62908	40S ribosomal protein S3	2.8	4.49E-03
P08730	Keratin, type I cytoskeletal 13	2.8	3.76E-02
Q6ZQA0	Neurobeachin-like protein 2	2.8	3.76E-02
P26638	Serine--tRNA ligase, cytoplasmic	2.4	3.10E-02
P42227	Signal transducer and activator of transcription 3	2.4	3.10E-02
Q9D154	Leukocyte elastase inhibitor A	2.4	2.75E-05
Q9Z1Q9	Valine--tRNA ligase	2.2	7.61E-05
Q8VCT3	Aminopeptidase B	2.0	1.48E-03
P84096	Rho-related GTP-binding protein RhoG	1.9	1.91E-03
P42932	T-complex protein 1 subunit theta	1.8	3.28E-02
O88593	Peptidoglycan recognition protein 1	1.8	4.31E-03
Q99KE1	NAD-dependent malic enzyme, mitochondrial	1.8	2.29E-02
O55029	Coatomer subunit beta′	1.7	1.49E-02
Q9EQH3	Vacuolar protein sorting-associated protein 35	1.7	9.63E-03
Q9CWJ9	Bifunctional purine biosynthesis protein PURH	1.6	1.48E-03
P80315	T-complex protein 1 subunit delta	1.5	2.40E-02
P19096	Fatty acid synthase	1.4	4.22E-03
P28293	Cathepsin G	1.3	1.72E-04
Q63844	Mitogen-activated protein kinase 3	1.2	3.10E-02
P60766	Cell division control protein 42 homolog	1.2	1.49E-02
Q8CCK0	Core histone macro-H2A.2	1.2	1.91E-03
Q9Z1Q5	Chloride intracellular channel protein 1	1.2	1.01E-02
Q9D8N0	Elongation factor 1-gamma	1.2	6.62E-03
Q91V92	ATP-citrate synthase	1.1	2.40E-02
P62827	GTP-binding nuclear protein Ran	1.0	1.15E-03